INVERSE PROBLEMS SOLUTION IN THE HYDRAULIC CHARACTERIZATION OF UNSATURATED SOILS

ZAVALA, M.[1*] – SAUCEDO, H.[2] – CASTANEDO, V.[3]

[1]*Unidad Académica de Ciencia y Tecnología de la Luz y la Materia, Universidad Autónoma de Zacatecas, Circuito Marie Curie S/N, Parque de Ciencia y Tecnología, Quantum, 98160 Zacatecas, México*

[2]*Comisión Nacional de Agua, Avenida Insurgentes Sur 2416, Copilco El Bajo, 04340 Ciudad de México, México*

[3]*Doctorado en Ingeniería, Universidad Nacional Autónoma de México, 04510 Ciudad de México, México*

**Corresponding author*
e-mail: mzavala73@uaz.edu.mx; phone: +52-49-2135-4512

(Received 10th Nov 2022; accepted 27th Feb 2023)

Abstract. Soil hydraulic characterization is fundamental to investigate water infiltration, redistribution and percolation in soils partially saturated. This work presents a mechanistic methodology of soils hydrodynamic characterization based on volumetric porosity, soil granulometric curve, a transient water flow event analysis in porous medium (vertical infiltration) and water volume drained by gravity effect. A numerical model based on one-dimensional Richards equation to describe vertical infiltration analysis is developed. The hydrodynamic characterization methodology for three types of soil is also applied.
Keywords: *granulometric curve, soil porosity, soil-water retention curve, hydraulic conductivity curve*

Introduction

The mechanistic description of water transfer processes in unsaturated soils requires precise knowledge of the hydraulic characteristics of porous medium. Of utmost important are the characteristic curve relating soil hydraulic conductivity K with the volumetric water content θ, and the soil-water retention curve relating volumetric water content θ with the soil water pressure head ψ. Generally, in hydrology and particularly in agricultural irrigation studies, the mathematical representation of these hydraulic characteristics is essential to analyze water infiltration, drainage, percolation, redistribution in the soil with Richards equation (Silva et al., 2019).

The specialized literature contains different models to describe the hydraulic properties of the soil, which vary conceptually and in sophistication (Assouline and Or 2013; Too, et al., 2014). That set of models covers pedotransfer functions (Tóth et al., 2015; Bohne, et al., 2019; Tian et al., 2021) and mechanicist models based on the Poiseuille and Laplace laws. The first group of models is established without explicitly considering the physical bases of water movement in the soil and the second group helps represent in detail the basic mechanisms of the process from laws of physics.

The mechanicist models most used in field and laboratory studies are those proposed by Brooks and Corey (1964), van Genuchten (1980) and Braddock et al. (2001). The popularity of these models is due to their ability to fit water retention experimental data (Du, 2020; Rastgou, et al., 2020), and also due to the fact that they can be easily

http://www.aloki.hu ● ISSN 1589 1623 (Print) ● ISSN 1785 0037 (Online)
DOI: http://dx.doi.org/10.15666/aeer/2102_17311747

combined with hydraulic conductivity models (e.g. Burdine, 1953; Mualem, 1976). However, some combinations of these models do not satisfy the fundamental infiltration properties (Fuentes et al., 1992), and the process to unify models is not closed. Therefore, research opportunities on the functional hydraulic properties and their behavior under different flow conditions remain open.

In hydrodynamic characteristics models, a series of parameters are involved that need to be estimated. Currently, there are different methodologies to determine them. These may vary in fundamental approach, complexity, cost, and precision. Different methods that exist for hydrodynamic characterization of unsaturated soils can be grouped into direct and inverse methods, and at the same time, laboratory or field. The latter method of hydraulic characterization of unsaturated soils is generally the most convenient; however, it is possible to achieve a good approximation of hydrodynamic properties in the lab by considering undisturbed soil samples taken in field.

Direct characterization methods consist on measuring infiltration rate, changes in moisture content and pressure potential in soil by using tensiometers and moisture sensors installed at different depths in soil profile while applying water on surface (Rezaie-Boroon et al., 2017; Smith and Kean, 2018; Le Roux and Jacobsz, 2021).

In recent years there have been great advances in electrical techniques to measure soil hydraulic properties. Among the most used devices are the TDR "Time domain reflectometer", electromagnetic induction devices, and underground penetrating radars, which have ability to provide measurements at great depths and at a large scale (Xiao et al., 2018; He et al., 2021); In addition, there are electromagnetic techniques such as optic fiber and electrochemical sensors that are mainly based on electrical conductivity measurements or dielectric constant measurements to determine moisture content.

In other ways there have been notable advances in sensors development to determine water pressure potential in soils and hydraulic conductivity, such as: osmotic tensiometers, heat dissipation units, electro-optical methods, ultracentrifuge methods (Joseph et al., 2022). However, direct measurement equipment has limitations such as requiring detailed calibration processes and high costs for most practical applications.

Inverse methods have become an excellent alternative to limitations of direct methods, with the basic premise of deducing the hydrodynamic properties of the soil from data that are more likely to be measured or more available. By definition, the solution to an inverse problem involves the determination of unknown causes based on observations of their effects, which contrasts with direct problem, whose solution requires finding the effects based on a description of their causes (Hopmans and Simunek, 1999).

A flexible way to solve an inverse problem is the use of parameter estimation techniques. In this method, the problem is presented by means of a differential equation subject to boundary conditions. By means of an appropriate numerical or analytical method, the equation is solved. The constitutive system functions are parameterized a priori, and coefficients are determined using an optimization algorithm applied to objective function.

Soil hydrodynamic properties can be estimated using inverse methods if an adequate representation of the studied system is made, since it is evident that any conceptual error in physical-mathematical model affects parameters estimation.

Infiltration and drainage experiments *in situ* or in laboratory can be carried out according to a well-established and theoretically supported methodology. In order to

http://www.aloki.hu ● ISSN 1589 1623 (Print) ● ISSN 1785 0037 (Online)
DOI: http://dx.doi.org/10.15666/aeer/2102_17311747

obtain quality information that allows studying and identifying soil-water retention parameters and unsaturated hydraulic conductivity of soils. In same sense, development of efficient numerical schemes based on nonlinear partial differential equations that describe the analyzed physical system is essential to evolve towards a higher stage of knowledge about hydrodynamic characteristics of partially saturated soils.

The aim of this work is to present a mechanistically based methodology for the hydrodynamic characterization of partially saturated soils. The methodology is based on porosity analysis and soil granulometric curve with the laws of Laplace, Stokes, and concepts of fractal geometry, as well as the analysis of inverse infiltration problems and drainage with Richards equation. The methodology was applied to determine hydraulic parameters of soil samples with contrasting hydraulic properties.

Materials and methods

Analytical representations of hydraulic properties of the unsaturated soils (soil-water retention curve and hydraulic conductivity curve), contain parameters to be determined, these can be grouped into *shape parameters* and *scale parameters.*

Shape parameters of hydraulic properties

According to Fuentes et al. (2001), it is possible to determine of the shape parameters that are in the unsaturated soils hydraulic properties from soil porosity and soil granulometric curve. Having Laplace's law and Stokes' law as a foundation and considering soil as a fractal object (Mandelbrot, 1982) and accepting similarity between the degree of saturation S(R) and accumulated frequency F(D), the following relationship is established between soil pores size (R) and soil particles diameter (D):

$$S(R) = F(D) \tag{Eq.1}$$

$$(R/R_d) = (D/D_g)^{1+\kappa} \tag{Eq.2}$$

where R_d is a characteristic parameter of pore size; D_g is a characteristic parameter of particle size. Exponent κ is estimated:

$$\kappa = \frac{2s-1}{2(1-s)} \tag{Eq.3}$$

where $s = D_f/E$, D_f is soil fractal dimension (D_f) and $E = 3$ is Euclidean dimension of physical space, defined implicitly as a function of the soil porosity ϕ:

$$(1-\phi)^s + \phi^{2s} = 1 \tag{Eq.4}$$

Transition from soil granulometric curve to soil-water retention curve $\theta(\psi)$ is carried out with *Equations 1–4*, considering that $\theta = \phi S(R)$ and $\theta = \phi F(D)$, where θ is the soil-water content and ψ is the pressure head in the soil. The procedure is valid for any functional model that represents the hydraulic properties of unsaturated soils.

http://www.aloki.hu ● ISSN 1589 1623 (Print) ● ISSN 1785 0037 (Online)
DOI: http://dx.doi.org/10.15666/aeer/2102_17311747

Analytical representations of the hydraulic properties

The analysis of the water movement in unsaturated soils requires representing the hydraulic properties of the soil by means of models that relate the hydraulic conductivity and the soil water tension in the soil as functions of the volumetric water content.

Fuentes et al. (1992) have shown that the soil-water retention curve model of van Genuchten (1980) subject to the Burdine (1953) constraint, combined with the hydraulic conductivity model of Brooks and Corey (1964) satisfy the integral properties of infiltration and recommend that this combination can be used in theoretical studies as well as field and laboratory studies (Stewart et al., 2013; Silva et al., 2019).

Van Genuchten's (1980) model is:

$$\theta(\psi) = \theta_r + (\theta_s - \theta_r)\left[1 + \left(\frac{\psi}{\psi_d}\right)^n\right]^{-m} \qquad m = 1 - 2/n \tag{Eq.5}$$

where θ_s and θ_r are the saturated and residual water contents $\left[L^3L^{-3}\right]$; ψ_d is a characteristic pressure value (scale parameter; L); m and n are dimensionless positive values (shape parameters).

Brooks and Corey's (1964) hydraulic conductivity curve is:

$$K(\theta) = K_s\left(\frac{\theta - \theta_r}{\theta_s - \theta_r}\right)^{\eta} \tag{Eq.6}$$

where η is a shape parameter empirical and positive; and K_s is the saturated hydraulic conductivity (scale parameter; LT^{-1}).

Shape parameters estimation that intervene in van Genuchten (*Eq. 5*) and Brooks and Corey (*Eq. 6*) models, m and η, is done from soil porosity (ϕ) and soil granulometric curve, and scale parameters (ψ_d and K_s) from reproduction with the numerical solution of one-dimensional Richards' equation, of infiltrated depth measured in infiltration and drainage tests in soil columns.

According to the van Genuchten model (*Eq. 5*), the experimental granulometric curves of the soils should be fitted with the following distribution function:

$$F(D) = \left[1 + (D_g/D)^N\right]^{-M} \tag{Eq.7}$$

According to relations (*Eqs. 1, 2* and *3*), transition from granulometric curve to retention curve for van Genuchten model (*Eq. 5*) allows to establish:

$$(MN/mn) \cong 1 + \kappa \tag{Eq.8}$$

where κ estimated with *Equation 3* and from Burdine restriction we have $m = 1 - 2/n$.

While shape parameter of hydraulic conductivity function can be estimated with the relationship deduced by Fuentes et al. (2001):

http://www.aloki.hu ● ISSN 1589 1623 (Print) ● ISSN 1785 0037 (Online)
DOI: http://dx.doi.org/10.15666/aeer/2102_17311747

$$\eta = 2s(2/\lambda + 1) \quad \text{(Eq.9)}$$

with $\lambda = mn$.

Scale parameters of the hydraulic properties

Soil hydrodynamic characterization can be completed by considering local or global infiltration experiments which allow obtaining information to identify the soil-water retention function scale parameters and of the unsaturated hydraulic conductivity. Point infiltration tests may consist of imposing a water head on soil surface and measuring the infiltrated depth evolution over time.

Vertical infiltration

Infiltration caused by a constant water head on surface of soil column can be described by one-dimensional Richards equation (1931):

$$C(\psi)\frac{\partial \psi}{\partial t} = \frac{\partial}{\partial z}\left[K(\psi)\left(\frac{\partial \psi}{\partial z} - 1\right)\right] \quad \text{(Eq.10)}$$

where ψ is the pressure head into the soil, expressed as the height of an equivalent water column $[L]$ (positive in saturated zones and negative in unsaturated zones); $C(\psi) = d\theta/d\psi$ is the specific capacity of soil $[L^{-1}]$; $K(\psi)$ is hydraulic conductivity $[LT^{-1}]$, in a saturated soil as a function of pressure potential; θ is the water volume per unit volume of soil or water content; $[L^3L^{-3}]$ is a function of ψ, known as the humidity characteristic curve or soil-water retention curve; gravitational potential is assigned to spatial coordinate "z" positively oriented down $[L]$.

The boundary conditions to describe one-dimensional infiltration caused by a water head on soil surface are:

$$\psi = \psi_{ini};\ 0 \le z \le P;\ t = 0 \quad \text{(Eq.11)}$$

$$\psi = h_w;\ z = 0;\ t > 0 \quad \text{(Eq.12)}$$

$$\frac{\partial(\psi - z)}{\partial z} = -1;\ z = P;\ t > 0 \quad \text{(Eq.13)}$$

where ψ_{ini} is the initial distribution of water pressure potential in soil; h_w is the water depth on surface of soil column; and P is column depth.

Numerical simulation model

Numerical solution of the *Equation 10* subject to *Equations 11, 12* and *13* has been performed with the finite element method (Zhu, 2018). In this method the dependent variable ψ is approximated by a linear combination of the fundamental functions φ_j defined by Kronecker's delta function:

http://www.aloki.hu ● ISSN 1589 1623 (Print) ● ISSN 1785 0037 (Online)
DOI: http://dx.doi.org/10.15666/aeer/2102_17311747

$$\psi(z,t) \cong \hat{\psi}(z,t) = \sum_{j=1}^{n} \varphi_j(z)\Psi_j(t) \quad \text{(Eq.14)}$$

where $\Psi_j(t)$ are time dependent coefficients and represent the approximate solution at specific points of a domain, "nodes" (n). Substituting the approximate solution $\hat{\psi}(z,t)$ in *Equation 10* generates an error or residual (ε) that can be written as:

$$\varepsilon = \hat{C}\frac{\partial\hat{\psi}}{\partial t} - \frac{\partial}{\partial z}\left[\hat{K}\frac{\partial(\hat{\psi}-z)}{\partial z}\right] \quad \text{(Eq.15)}$$

This residual is minimized by forming a weighted integral of ε over the solution domain (0,P) and requiring that the integral, called weighted residual, be zero:

$$\int_0^P \varepsilon v_i(z)dz = \int_0^P \left\{\hat{C}\frac{\partial\hat{\psi}}{\partial t} - \frac{\partial}{\partial z}\left[\hat{K}\frac{\partial(\hat{\psi}-z)}{\partial z}\right]\right\} v_i(z)dz = 0 \quad \text{(Eq.16)}$$

where $v_i(x)$, with $i = 1,...,n$, are weight functions.

Integration by parts of *Equation 16* led to:

$$\int_0^P \hat{C}\frac{\partial\hat{\psi}}{\partial t}v_i dz + \int_0^P \hat{K}\left(\frac{\partial\hat{\psi}}{\partial z} - 1\right)\frac{dv_i}{dz}dz = \hat{K}\frac{\partial(\hat{\psi}-z)}{\partial z}v_i\Big|_0^P \quad \text{(Eq.17)}$$

With the substitution of finite element solution $\hat{\psi}$ given by *Equation 14* in *Equation 17*, considering that weight functions are equal to the basic functions $v = \varphi$ (Galerkin's method) and assuming a linear variation of hydraulic properties in element ($\hat{C} = \varphi_g C_g$ and $\hat{K} = \varphi_g K_g$), the following system of ordinary differential equations was obtained:

$$[A]\frac{d\{\Psi\}}{dt} + [B]\{\Psi\} = \{F\} + \{G\} \quad \text{(Eq.18)}$$

where A is a mass matrix, B is the rigidity matrix, F is the vector that contain values or flow ratios in the boundary ($z = 0$ and $z = P$) and G is the gravity vector. Using linear interpolation functions, coefficients of these matrices and vectors were calculated, resulting:

$$A_{ij} = \sum_{j=1}^{n}\int_0^P C_g\overline{\varphi}_g\overline{\varphi}_i\overline{\varphi}_j dz = \delta_{ij}\sum_e C_j\frac{\Delta z}{2} \quad \text{(Eq.19)}$$

$$B_{ij} = \sum_{j=1}^{n}\int_0^P K_g\varphi_g\frac{d\varphi_i}{dz}\frac{d\varphi_j}{dz}dz = \sum_e (-1)^{i+j}\frac{\overline{K}}{\Delta z} \quad \text{(Eq.20)}$$

http://www.aloki.hu ● ISSN 1589 1623 (Print) ● ISSN 1785 0037 (Online)
DOI: http://dx.doi.org/10.15666/aeer/2102_17311747

$$F_i = \hat{K}\frac{\partial(\hat{\psi}-z)}{\partial z}\varphi_i\Big|_0^p = \begin{cases} E(t) & ; \quad i=1 \quad (z=0) \\ q_d & ; \quad i=n \quad (z=P) \end{cases} \tag{Eq.21}$$

$$G_i = \int_0^p K_g \varphi_g \frac{d\varphi_i}{dz} dz = \sum_e \overline{K} \begin{bmatrix} 1 \\ -1 \end{bmatrix} \tag{Eq.22}$$

where φ are the basic functions of concentrated mass system (Neuman, 1973); δ_{ij} is Kronecker's delta; $\overline{K}$ is hydraulic conductivity in element taken as arithmetic average of conductivities in the two nodes of the element "e" (as a consequence of the form adopted for base functions); E represents evaporation intensity on ground surface or rainfall intensity; and q_d is drained water flow.

Time derivative approximation in *Equation 18* was performed with following discretization scheme:

$$\left(\frac{d\{\Psi\}}{dt}\right)^{t+\omega\Delta t} = \frac{\{\Psi\}^{t+\Delta t} - \{\Psi\}^t}{\Delta t} \tag{Eq.23}$$

$$\{\Psi\}^{t+\omega\Delta t} = \omega\{\Psi\}^{t+\Delta t} + (1-\omega)\{\Psi\}^t \tag{Eq.24}$$

where Δt is time step and ω is a time weighting coefficient ($0 \le \omega \le 1$), taken as $\omega = 1$ (implicit scheme). Substituting *Equations 23* and *24* in *Equation 18* and applying Picard's linearization method, is obtained:

$$\left[\frac{A^w_{t+\omega\Delta t}}{\Delta t} + \omega B^w_{t+\omega\Delta t}\right]\{\Psi\}^{w+1}_{t+\omega\Delta t} = \left[\frac{A^w_{t+\omega\Delta t}}{\Delta t} - (1-\omega)B^w_{t+\omega\Delta t}\right]\{\Psi\}_t + \{F\}^w_{t+\omega\Delta t} + \{G\}^w_{t+\omega\Delta t} \tag{Eq.25}$$

where w indicates the iteration number in time interval. System (*Eq.25*) is solved using a preconditioned conjugate gradient iterative method (Noor and Peters, 1987) that allows to eliminate rounding errors associated with backward substitution procedure required in direct methods. The numerical scheme was coded in the C++ programming language.

Soil columns and experimental tests

To develop the study, three disturbed soil samples with different hydraulic properties were obtained from an agricultural area in the state of Morelos, Mexico. The area is located in the Amacuzac River hydrological basin, between parallels 18° 20' and 19° 07' north latitude and between 98° 38' and 99° 31' west longitude. The samples collected with a manual auger were taken to the laboratory, where they were dried, organic matter was eliminated, each one was sieved independently. Granulometric curves were determined by applying Bouyoucos procedure for solid particles smaller than 74 microns, while particles distribution between 74 and 2000 microns was done applying sieving method. To identify them, each soil sample was assigned a typical name of the place where they were obtained. The textural classification was carried out

http://www.aloki.hu ● ISSN 1589 1623 (Print) ● ISSN 1785 0037 (Online)
DOI: http://dx.doi.org/10.15666/aeer/2102_17311747

applying the USDA criteria, the soil called Cuaculan was classified as sand, Sta. Maria is loam and La Pintura is clay loam.

In the laboratory three acrylic columns with a length $P = 75\ cm$ and a circular cross-section of diameter $D_c = 15\ cm$, with a porous plate covered by a filter placed in its lower part with the purpose of retaining of the soil, were manufactured. Each soil sample was placed inside the column in 10 cm thick layers, trying to keep the bulk density constant to generate homogeneous conditions. The initial water content (θ_{ini}) was determined in each column and an infiltration test was carried out, applying a constant water head on its surface (h_w) and measuring the depth of the infiltrated water over time (*Fig. 1*). Once the soil columns were saturated, the surface water head was removed and the bottom of the column was covered until the soil water pressure in the soil stabilized. Finally, the surface of the column was covered with plastic to eliminate evaporation and the bottom of the column was cut open to measure the volume of water drained over time.

Figure 1. *Soil columns*

Results and discussion

Case 1: Hydraulic characterization of the three soils

To illustrate the methodology described, the estimation of the hydraulic parameters of three soils was carried out.

Shape parameters

Soil porosity of each column (ϕ) is estimated with classic relation $\phi = 1 - \rho_a / \rho_s$, where ρ_a is dry soil volumetric density and ρ_s solid particles density ($\rho_s = 2.65\ g/cm^3$ of quartz particles). Introducing soil porosity values in *Equation 4* the function was solved using Newton-Raphson method (Burden et al., 2015), corresponding values of relative dimension s for each soil are obtained. Finally, according to Haverkamp et al. (2005) water volumetric content at saturation θ_s can be assimilated to total volumetric

http://www.aloki.hu ● ISSN 1589 1623 (Print) ● ISSN 1785 0037 (Online)
DOI: http://dx.doi.org/10.15666/aeer/2102_17311747

porosity of soil $\theta_s = \phi$, which implies that 100% of soil pores are filled with water; while volumetric residual water content can be assumed equal to zero $\theta_r = 0$, if it is accepted that soil water content in soil tends to zero when the absolute value of water pressure potential tends to infinity, that is $\theta \to 0$, when $|\psi| \to \infty$. Parameters calculated following the procedure described are presented in *Table 1*.

Experimental granulometric curves are fitted with *Equation 7*, using a nonlinear optimization algorithm and the coefficient of determination R^2. Results obtained for each soil sample are presented in *Figures 2*, *3* and *4*.

Table 1. *Physical and volumetric parameters of three soils. ρ_a is the bulk density; ϕ is the soil porosity; s is the relative dimension; θ_s is the saturated water content and θ_r is the residual water content*

Soil	ρ_a cm^3/cm^3	ϕ cm^3/cm^3	s	θ_s cm^3/cm^3	θ_r cm^3/cm^3
Cuaculan sand	1.62	0.390	0.671	0.390	0.000
Sta. María loam	1.02	0.614	0.719	0.614	0.000
La Pintura clay loam	1.33	0.509	0.696	0.509	0.000

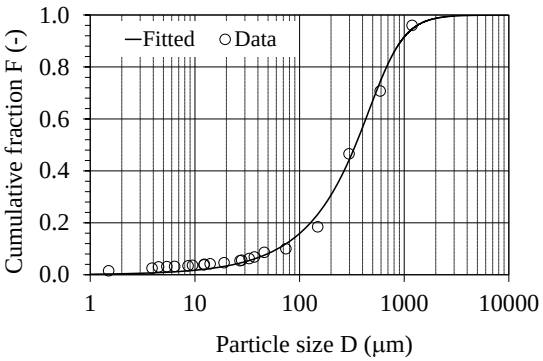

Figure 2. *Granulometric curve of Cuaculan sand and adjustment function F(D) with* $D_g = 675\,\mu m$ *and* $M = 0.325$ *(*$R^2 = 0.9933$*)*

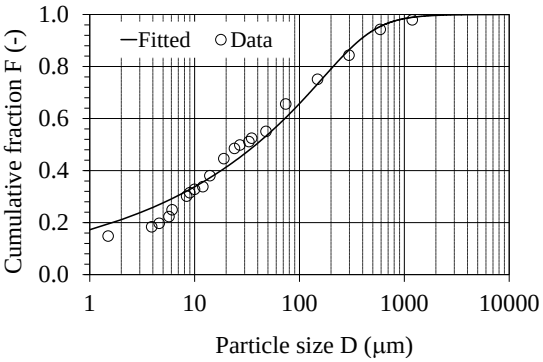

Figure 3. *Granulometric curve of Sta. María loam and adjustment function F(D) with* $D_g = 415\,\mu m$ *and* $M = 0.127$ *(*$R^2 = 0.9699$*)*

http://www.aloki.hu ● ISSN 1589 1623 (Print) ● ISSN 1785 0037 (Online)
DOI: http://dx.doi.org/10.15666/aeer/2102_17311747

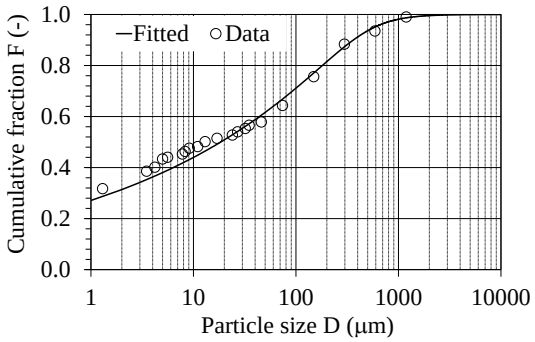

Figure 4. *Granulometric curve of La pintura clay loam and adjustment function F(D) with* $D_g = 500\,\mu m$ *and* $M = 0.095$ *(*$R^2 = 0.9793$*)*

The κ parameter was estimated using the *Equation 3* and from *Equation 8* and Burdine restriction ($m = 1 - 2/n$) the parameters m and n of the soil-water retention curve were estimated. While form parameter of conductivity function can be estimated with the relationship *Equation 9*. Results obtained for each soil column are presented in *Table 2*.

Table 2. *Shape parameters.* κ *is the exponent of Equation 3; M, N, are de exponent of Equation 7; m, n, are de exponent of the van genuchten model (Eq. 5); y* η *is the exponent of the Broks and Corey model (Eq. 6)*

Soil	κ	M	N	m	n	η
Cuaculan sand	0.522	0.325	2.963	0.240	2.633	5.586
Sta. María loam	0.781	0.127	2.291	0.076	2.164	19.080
La Pintura clay loam	0.646	0.095	2.210	0.060	2.128	23.218

Scale parameters estimation

Hydraulic characteristics of scale parameters (ψ_d and K_s) are estimated by reproducing, with the developed simulation model, the evolution of the measured infiltrated water depth in experimental tests over time. Infiltration tests characteristics are presented in *Table 3*.

Table 3. *Initial condition and upper boundary condition in infiltration tests*

Data	Cuaculan sand	Sta. Maria loam	La Pintura clay loam
Hydraulic head on surface column h_w (cm)	3.0	10.0	6.5
Initial water volumetric content θ_{ini} (cm^3/cm^3)	0.008	0.013	0.015

To reproduce infiltration tests, numerical solution (*Eq. 25*) is used. The solution domain is discretized with a uniform finite element mesh of 751 nodes distributed in 750 elements ($\Delta z = 0.1 cm$). Initial time step chosen was that it increases during simulation by 5% up to a maximum value of 60 s if the number of iterations required to solve system (20) in the time interval is less than 5.

http://www.aloki.hu ● ISSN 1589 1623 (Print) ● ISSN 1785 0037 (Online)
DOI: http://dx.doi.org/10.15666/aeer/2102_17311747

Numerical model is used with estimated values m, η, θ_s and θ_r, values of ψ_d and K_s were calibrated in order to reproduce experimental observations; results obtained are presented in *Figures 5*, *6* and *7*.

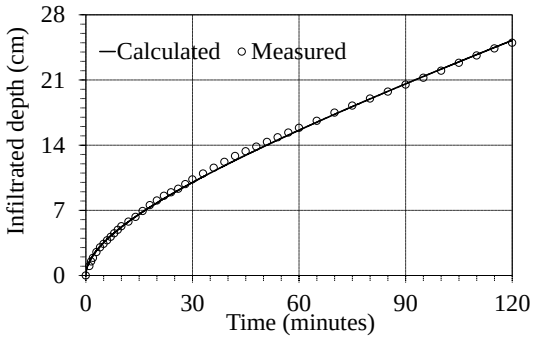

Figure 5. *Comparison of measured water infiltrated depth and calculated water infiltrated depth with:* $\psi_d = -19.5\,\text{cm}$ *and* $K_s = 7.6\,\text{cm/h}$ *;* $R^2 = 0.9979$ *(Cuaculan sand)*

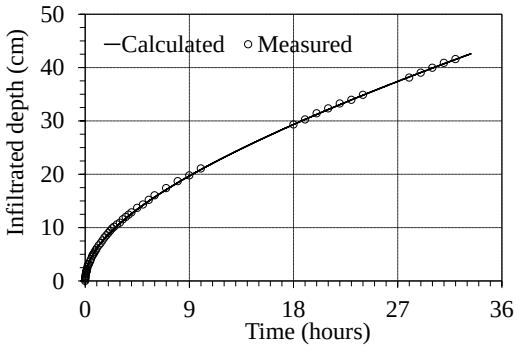

Figure 6. *Comparison of measured water infiltrated depth and calculated water infiltrated depth with:* $\psi_d = -45.5\,\text{cm}$ *and* $K_s = 0.51\,\text{cm/h}$ *;* $R^2 = 0.9991$ *(Sta. María loam)*

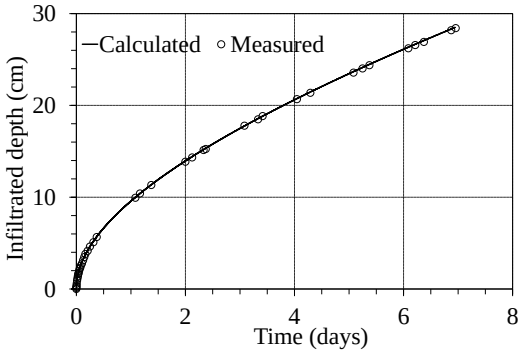

Figure 7. *Comparison of measured water infiltrated depth and calculated water infiltrated depth with:* $\psi_d = -51.0\,\text{cm}$ *and* $K_s = 0.06\,\text{cm/h}$ *;* $R^2 = 0.9993$ *(La Pintura clay loam)*

In order to close the soil's hydrodynamic characterization, the capillary hysteresis phenomenon must be considered (Berlotti and Mayergoys, 2006), which causes that,

http://www.aloki.hu ● ISSN 1589 1623 (Print) ● ISSN 1785 0037 (Online)
DOI: http://dx.doi.org/10.15666/aeer/2102_17311747

retention curves corresponding to drainage and infiltration to be different. It occurs due to differences present in processes of emptying or filling pores of soil. There are several models in the literature to predict the retention curve for drainage (drying curve), there are empirical models (Chen, 2020; Capparelli and Spolverino, 2020) and also theoretical models that use the water retention curve for infiltration (Kargas et al., 2021) and others that directly consider drainage tests to derive this curve (Shein and Mady, 2018). However, the curve for drainage can be directly determined from the total water depth that drains initially saturated soil column with zero evaporation on its surface $(\ell_{d\max})$.

When time of drainage $t \to \infty$, Darcy's flow tends to zero throughout the soil column, pressure distribution tends to hydrostatic equilibrium conditions:

$$\psi(z,\infty) = z - P \qquad \text{(Eq.26)}$$

Consequently, maximum drained infiltrated depth is provided by:

$$\ell_{d\max} = \int_0^P [\theta_s - \theta(z,\infty)]dz \qquad \text{(Eq.27)}$$

The use of *Equation 5,* considering equation *Equation 26,* in *Equation 27* allows to obtain:

$$\ell_{d\max} = (\theta_s - \theta_r)\left[P - |\psi_d| \int_0^{P/|\psi_d|} (1+\psi_*^n)^{-m} d\psi_*\right] \qquad \text{(Eq.28)}$$

As shape parameters of soil hydraulic properties m, n, and η, and volumetric water contents θ_s and θ_r have been estimated independently of transient water flow events in soil column, it can be considered that these are the same for infiltration and drainage. Additionally, capillary hysteresis in hydraulic conductivity curve is negligible in various types of soil and its effect is bigger in soil-water retention curve (Mualem, 1976), therefore hydraulic conductivity at saturation estimated for infiltration can be assumed equal for drainage processes, that is $K_{s(inf)} = K_{s(dren)}$. Consequently, the effect of capillary hysteresis can be absorbed by the scale parameter ψ_d. With previously obtained parameter values and considering the maximum depth of water drained measured in each soil column $(\ell_{d\max})$, *Equation 25* was solved to determine ψ_d values for drying. Values are: Cuaculan sand $\psi_{d(dry)} = -32.80$ cm, Sta. Maria loam $\psi_{d(dry)} = -46.00$ cm and La Pintura clay loam $\psi_{d(dry)} = -63.00$ cm.

Case 2: Comparison with another characterization method

To show the goodness of the proposed characterization methodology (P.C.M.), we analyze the shape parameters of the solil-water retention curve and compare them with those obtained with the direct characterization method established in the literature (D.C.M.). The direct method consists of collecting a soil sample and determining the experimental soil-water retention curve with devices and/or sensors and adjusting it with a functional model, in this case *Equation 5* is used.

http://www.aloki.hu ● ISSN 1589 1623 (Print) ● ISSN 1785 0037 (Online)
DOI: http://dx.doi.org/10.15666/aeer/2102_17311747

In the comparison, widely used soils in the literature in validation processes were used (Stewart et al., 2013; Kargas et al., 2022). Two soils with contrasting hydraulic properties, "Grenoble 1 sand" and "Yolo light clay" were selected and their data correspond to the values reported in the UNSODA 2.0 (Nemes et al., 1999) and presented in *Table 4*.

Table 4. *Physical and volumetric parameters of two soils.* ρ_a *is the bulk density;* ϕ *is the soil porosity;* θ_s *is the saturated water content;* θ_r *is the residual water content*

Soils	ρ_a cm^3/cm^3	ϕ cm^3/cm^3	θ_s cm^3/cm^3	θ_r cm^3/cm^3
Grenoble 1 sand	1.510	0.430	0.362	0.000
Yolo light clay	1.319	0.502	0.495	0.000

Applying the direct estimation method (D.C.M.), the soil-water retention data reported in the database UNSODA 2.0 was adjusted with *Equation 5*, the results are presented in *Figures 8* and *9*.

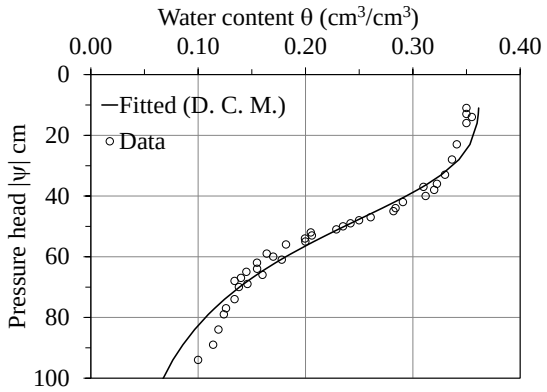

Figure 8. *Soil-water retention curve of Grenoble 1 sand and adjustment function Equation 5 with* $\psi_d = -47.5\text{cm}$ *and m = 0.528 (*$R^2 = 0.9749$*)*

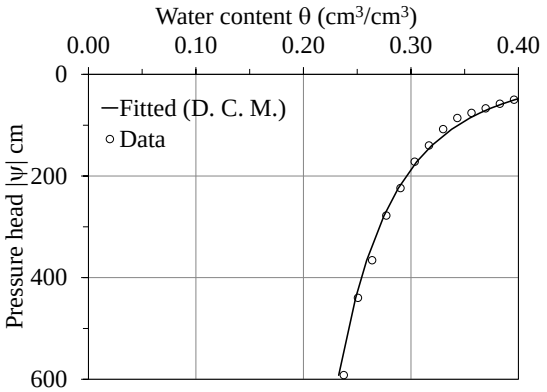

Figure 9. *Soil-water retention curve of Yolo light clay and adjustment function Equation 5 with* $\psi_d = -19.2\text{cm}$ *and* $m = 0.099$ *(*$R^2 = 0.9947$*)*

http://www.aloki.hu ● ISSN 1589 1623 (Print) ● ISSN 1785 0037 (Online)
DOI: http://dx.doi.org/10.15666/aeer/2102_17311747

The experimental granulometric curves were fitted with *Equation 7* and the results are presented in *Figures 10* and *11*.

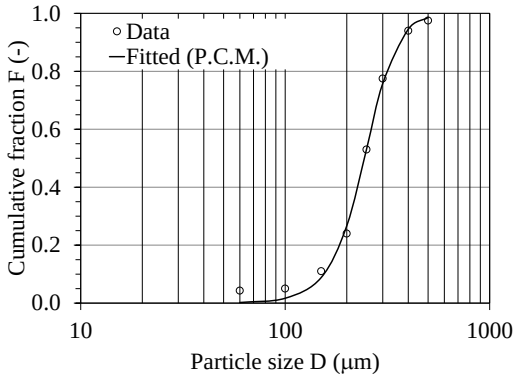

Figure 10. *Granulometric curve of Grenoble 1 sand and adjustment function Equation 7 with* $D_g = 268.6\,\mu m$ *and* $M = 0.674$ *(* $R^2 = 0.9977$ *)*

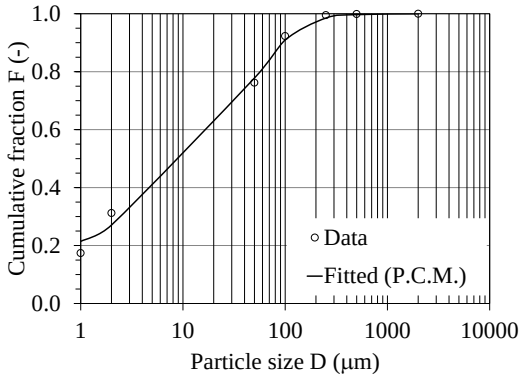

Figure 11. *Granulometric curve of Yolo light clay and adjustment function Equation 7 with* $D_g = 97.1\,\mu m$ *and* $M = 0.144$ *(* $R^2 = 0.9948$ *)*

Applying the *Equations 3, 4* and *8* the shape parameters of the corresponding retention curves were estimated (P.C.M.). *Table 5* shows the values of the parameters obtained with both characterization procedures, the results are acceptably close, with the advantage that the proposed method is easy to apply and does not require complex and expensive sensors or devices. The differences between the obtained values can be absorbed by the scale parameters of the soil hydraulic curves when they are determined in the modeling of the infiltration test that is required to complete the characterization procedure.

Table 5. *Shape parameters (m and n) of the van Genuchten retention curve (Eq. 5) obtained with the direct characterization method (D.C.M.) and with the proposed characterization method (P.C.M.)*

Soil	**D.C.M. m**	**D.C.M n**	**P.C.M. m**	**P.C.M. n**
Grenoble 1 sand	0.528	4.235	0.570	4.649
Yolo light clay	0.099	2.220	0.093	2.206

http://www.aloki.hu ● ISSN 1589 1623 (Print) ● ISSN 1785 0037 (Online)
DOI: http://dx.doi.org/10.15666/aeer/2102_17311747

Conclusions

A simple and precise methodology for soil hydraulic characterization based on laws of Laplace, Poiseuille, Stokes, fractal geometry, and a numerical solution of the one-dimensional Richards equation has been presented. This methodology has been applied to hydrodynamic characterization of disturbed soil samples and laboratory conditions considering a combination of moisture retention and hydraulic conductivity curves that satisfy the integral properties of infiltration.

This methodology can be applied to characterize homogeneous soils through infiltration tests carried out with the double cylinder infiltrometer method. In this method, one-dimensional infiltration is induced in the area of influence of the inner cylinder. The methodology can also be applied to other analytical representations of soil hydraulic properties, deriving the calculation relationships of the shape parameters of the soil-water retention curve and hydraulic conductivity curve considering *Equations 1*, *2*, *3* and *4*.

REFERENCES

[1] Assouline, S., Or, D. (2013): Conceptual and parametric representation of soil hydraulic properties: a review. – Vadose Zone Journal 12: 1-20.
[2] Berlotti, G., Mayergoys, I. (2006): The Science of Hysteresis. – Elsevier Academic Press, Great Britain.
[3] Bohne, K., Renger, M., Wessolek, G. (2019): New pedotransfer function ("CRC") for the prediction of unsaturated soil hydraulic conductivity using soil water retention data. – International Agrophysics 33: 503-510.
[4] Braddock, R. D., Parlange, J. - Y., Lee, H. (2001): Application of a soil water hysteresis model to simple water retention curves. – Transport in Porous Media 44: 407-420.
[5] Brooks, R. H., Corey, A. T. (1964): Hydraulic properties of porous media. – Hydrology Paper 3, Colorado State University, Fort Collins.
[6] Burden, R. L., Faires, J. D., Burden, A. M. (2015): Numerical Analysis. – Brooks/Cole Pub Co. Pacific Grove, CA.
[7] Burdine, N. T. (1953): Relative permeability calculation from size distribution data. – Transactions of the American Institute of Mining and Metallurgical Engineers 198: 71-78.
[8] Capparelli, G., Spolverino, G. (2020): An empirical approach for modeling hysteresis behavior of pyroclastic soils. – Hydrology 7: 1-14.
[9] Chen, Y. (2020): Soil-water retention curves derived as a function of soil dry density. – GeoHazards 1: 3-19.
[10] Du, C. (2020): Comparison of the performance of 22 models describing soil water retention curves from saturation to oven dryness. – Vadose Zone J. 19: e20072: 1-20.
[11] Fuentes, C., Haverkamp, R., Parlange, J. - Y. (1992): Parameter constraints on closed-form soilwater relationships. – Journal of Hydrology 134: 117-142.
[12] Fuentes, C., Brambila, F., Vauclin, M., Parlange, J. - Y., Haverkamp, R. (2001): Modelación de la conductividad hidráulica de los suelos no saturados. – Ingeniería Hidráulica en México 16(2): 119-137.
[13] Haverkamp, R., Leij, F. J., Fuentes, C., Sciortino, A., Ross, P. J. (2005): Soil water retention. I: Introduction of a Shape Index. – Soil Science Society of American Journal 69: 1881-1890.
[14] Hea, H., Aoguabc, K., Li, M., Xu, J., Sheng, W., Jones, S. B., González-Teruel, J. D., Robinson, D. A., Horton, R., Bristow, K., Dyck., M., Filipovićk, V., Noborio, K., Wu, Q.,

http://www.aloki.hu ● ISSN 1589 1623 (Print) ● ISSN 1785 0037 (Online)
DOI: http://dx.doi.org/10.15666/aeer/2102_17311747

Jin, H., Feng, H., Si, B. S., Lv, J. (2021): A review of time domain reflectometry (TDR) applications in porous media. – Advances in Agronomy 168: 83-155.

[15] Hopmans, J. W., Šimůnek, J. (1999): Review of Inverse Estimation of Unsaturated Hydraulic Properties. – In: van Genuchten, M. T., Leij, F., Wu, L. (eds.) Proc. Int. Workshop on the Characterization and Measurement of the Hydraulic Properties of Unsaturated Porous Media, Riverside, CA, 22-24 Oct 1997. University of California, Riverside, CA, pp. 643-655.

[16] Joseph, J., Rakshith, S., Singh, D. N., Tang, C. S. (2022): MI-ECku: A novel methodology for estimating unsaturated hydraulic conductivity of porous media. – Acta Geotechnica 17: 3855-3865.

[17] Kargas, G., Soulis, K. X., Kerkides, P. (2021): Implications of hysteresis on the horizontal soil water redistribution after infiltration. – Water 13: 2773: 1-21.

[18] Kargas, G., Koka, D., and Londra, P. A. (2022): Determination of soil hydraulic properties from infiltration data using various methods. – Land 11(779): 1-16.

[19] Le Roux, P. F., Jacobsz, S. W. (2021): Performance of the tensiometer method for the determination of soil-water retention curves in various soils. – Geotechnical Testing Journal 44(6): 20200196.

[20] Mandelbrot, B. (1982): The Fractal Geometry of Nature. – W. H. Freeman and Company, New York.

[21] Mualem, Y. (1976): A new model for predicting the hydraulic conductivity of unsaturated porous media. – Water Resources Research 12: 513-522.

[22] Nemes, A., Schaap, M. G., Leij, F. J. (1999): The UNSODA: Unsaturated Soil Hydraulic Database, Version 2.0. – Salinity Laboratory, Riverside, CA.

[23] Neumann, S. P. (1973): Saturated-unsaturated seepage by finite elements. – Journal of the Hydraulics Division, American Society of Civil Engineers, HY12, Paper 10201: 2233-2250.

[24] Noor, K. A., Peters, J. M. (1987): Preconditioned conjugate gradient technique for the analysis of symmetric structures. – International Journal of Numerical Methods in Engineering 24: 2057-2070.

[25] Rastgoua, M., Bayatb, H., Mansoorizadehc, M., Gregory, A. S. (2020): Estimating the soil water retention curve: comparison of multiple nonlinear regression approach and random forest data mining technique. – Computers and Electronics in Agriculture 174: 105502: 1-13.

[26] Rezaie-Boroon, M. H., Acosta, O., Chipres, R., Cox, C., Diemel, F., Ho, N., Li, S., Lopez, R., Luque, M., Martinez, M., Palacios, D., Wright, J. (2017): Water flow path characterization in shallow vadose zone using tensiometers. – Journal of Water Resource and Protection 9: 1082-1096.

[27] Richards, L. A. (1931): Capillary conductions of liquids through porous medium. – Physics 1: 318-333.

[28] Shein, E. V., Mady, A. Y. (2018): Hysteresis of the water retention curve: wetting branch simulation based on the drying curve. – Moscow University Soil Science Bulletin 73: 124-128.

[29] Silva, U. B., Gico Lima Montenegro, S. M., Paiva Coutinho, A., Rabelo Coelho, V. H., dos Santos Araújo, D. C., Villar Gusmão, A. C., dos Santos Neto, S. M., Lassabatere, L., Angulo-Jaramillo, R. (2019): Modelling soil water dynamics from soil hydraulic parameters estimated by an alternative method in a tropical experimental basin. – Water 11(5): 1007: 1-19.

[30] Smith, J. B., Kean, J. W. (2018): Long-term soil-water tension measurements in semiarid environments: a method for automated tensiometer refilling. – Vadose Zone J. 17(180070): 1-5.

[31] Stewart, R. D., Rupp, D. E., Abou Najm, M. R., Selker, J. S. (2013) Effect of initial soil moisture on sorptivity & infiltration. – Water Resources Research 49: 7037-7047.

http://www.aloki.hu ● ISSN 1589 1623 (Print) ● ISSN 1785 0037 (Online)
DOI: http://dx.doi.org/10.15666/aeer/2102_17311747

[32] Tian, Z., Chen, J., Cai, C., Gao, W., Ren, T., Heitman, J. L., Horton, R. (2021): New pedotransfer functions for soil water retentions curves than better account for bulk density effects. – Soil and Tillage Research 205: 104812.
[33] Too, V. K., Omuto, C. T., Biamah, E. K., Obiero, J. P. (2014): Review of soil water retention characteristic (SWRC) Models between saturation and oven dryness. – Open Journal of Modern Hydrology 4: 173-182.
[34] Tóth, B., Weynants, M., Nemes, A., Makó, A., Bilas, G., Tóth, G. (2015): New generation of hydraulic pedotransfer functions for Europe. – European Journal of Soil Science 66: 226-238.
[35] Van Genuchten, M. T. (1980): A closed-form equation for predicting the hydraulic conductivity of the unsaturated soils. – Soil Science Society of American. Journal 44: 892-898.
[36] Xiao, X., Guan, B., Ihamouten, A., Villain, G., Dérobert, X., Tian., G. (2018): Monitoring water transfers in limestone building materials with water retention curve and ground penetrating radar: a comparative study. – NDT&E International 100(December): 31-39.
[37] Zhu, B. (2018): The Finite Element Method: Fundamentals and Applications in Civil, Hydraulic, Mechanical and Aeronautical Engineering. – John Wiley & Sons, Singapore.

http://www.aloki.hu ● ISSN 1589 1623 (Print) ● ISSN 1785 0037 (Online)
DOI: http://dx.doi.org/10.15666/aeer/2102_17311747